

(Submitted to the 7th Int. Workshop on Anomalies in Hydrogen/Deuterium Loaded Metals, Sept. 2006)

## Fusion Rates of Bosonized Condensates

Akito Takahashi <sup>\*1, \*2</sup> and Norio Yabuuchi <sup>\*1</sup>

<sup>\*1</sup>; High Scientific Research Laboratory, <sup>\*2</sup>: Osaka University  
akito@sutv.zaq.ne.jp

**Abstract:** In Part-I, theoretical basis for formulating fusion rates in condensed matter is summarized. Nuclear strong interaction, S-matrix, T-matrix, fusion rate for steady state dde\* molecule as bosonized condensate, and fusion rate formula for collision process are briefly given.

In Part-II, application for TSC-induced fusion is summarized. Fusion rate formulas for adiabatic approach in EQPET theory are summarized. Final state interaction is briefly discussed. Time-dependent approach for TSC squeezing motion is briefly introduced.

### Part-I: Basic Theory

#### 1.1 Nuclear Potential

In general, nuclear reaction is usually theorized and analyzed in three steps: initial state interaction, intermediate compound state and final state interaction. Transition from intermediate state to final state has various, sometimes complex, channels such as the electro-magnetic transition to ground state emitting gamma rays, the particle (neutron, proton, alpha-particle etc.) emission and residual nucleus, which sometimes decay to ground state emitting gamma-rays, and the direct break-up to two or more nuclei like fission. Potential for nuclear strong force and Coulomb force in these cases can be categorized into three cases<sup>1)</sup> of Fig.1-1.

The potential state (I) shows the case that nucleons (neutrons and protons) are trapped in a very deep well of strong force. Stable isotopes of masses less than 60 have this type potential well. Fusion reactions by two light nuclei produce stable isotopes of this type.

The potential state (II) appears for intermediate compound state in general. Radioactive isotope has this kind of potential. Stable isotopes having masses greater than 60 are trapped in these type potentials which are drawn according to the fission channels breaking-up to lighter nuclei. In this case, the depth of trapping potential is deep enough to have very long life time, but positive Q-value for fission channels makes height of potential tail in outer-skirt lower than the depth of trapping well. At ground state, the thickness of potential well is large enough to make the quantum-mechanical tunneling probability of fission to be “inverse-astronomically” very close to zero.

Therefore, nucleus is regarded as stable isotope. Here, Q-value is obtained by calculating mass defect between before and after reaction, using Einstein's formula  $E = mc^2$ . However, when the intermediate compound nucleus has high inner excited energy  $E_x$ , the thickness of outer wall of trapping potential becomes relatively thin and quantum mechanical tunneling probability for particle emission or fission can

dramatically increase. Fission process for uranium and trans-uranium nuclei is induced in this way. Moreover, we may have possibility of fission for lighter nuclei with mass  $A < 200$ . In some of proposed theories<sup>2-4)</sup> in the Condensed Matter Nuclear Science (CMNS), deterministic models of fission for  $60 < A < 200$  nuclei have been developed.

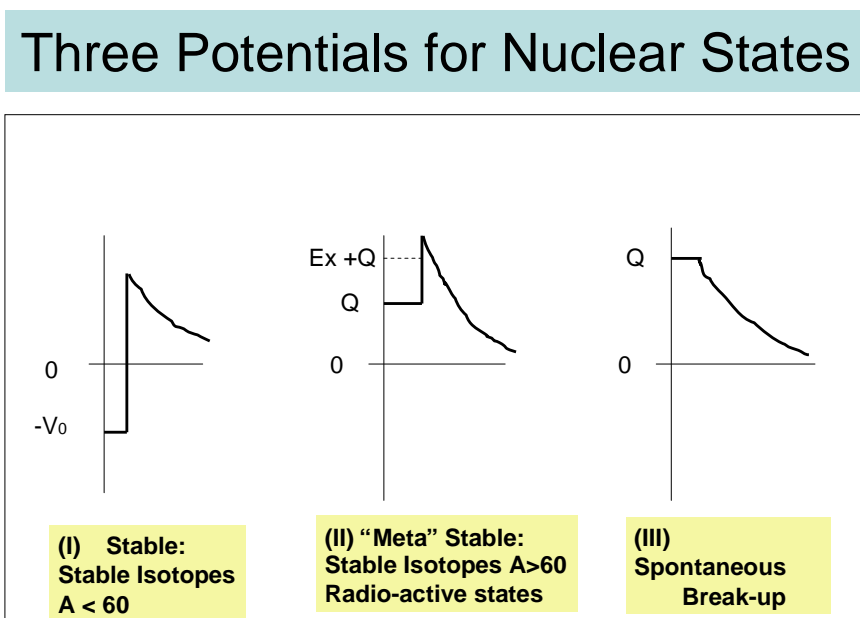


**Fig.1-1: Three potential types for nuclear interaction**

The potential type (III) is the case for intermediate compound nucleus having very high inner excited energy  $Ex$ , such as cases of fusion reactions of hydrogen isotopes. Compound nucleus in this case promptly breaks up to fragment-particles.

### 1.2 Strong Interaction

Now we explain very briefly the feature of potential by nuclear strong interaction. The reason why nucleons are trapped within very small spherical space with radius about 5 fm ( $1 \text{ fm} = 10^{-15} \text{ m}$ ) was first solved by the famous Yukawa model of pion exchange. Hideki Yukawa won Nobel Prize by this theory. Later, the theory of strong force has been deepened by the development of QCD<sup>5)</sup> based on concept of quark and gluon. However, as the conclusion in recent views of nuclear physics, the strong interaction can be drawn accurately enough by the Yukawa model with charged pions ( $\pi^+$ ,  $\pi^-$ ) and neutral pion, for relative reaction energy less than about 200 MeV (less than the threshold energy of pion-generation). Especially, for fusion reaction process, charged pions play role of sticking two (or more) nuclei.

Nuclear fusion by strong interaction can be simulated by the catch-ball model of charged pions between nuclei for fusing. Due to the very short range of de Broglie wave length (bout 2 fm) of pion, the strong interaction for fusion becomes very short range force, namely "almost on surface" sticking force. For example, when relatively large ( $A > 6$ ) two nuclei approach closely, fusion force by exchanging charged pions (between

neutron and proton for counter-part nuclei) becomes the sticking force near at surface ( $R=r_0$ ). Exchange of neutral pion for scattering (repulsive) force between nucleons of counter-part nuclei also happens in the region relatively near at surface.

Especially, nuclear fusion reactions at very low energy as cold cluster fusion and transmutation as modeled by EQPET/TSC theory (see Part II), largeness of surface area for exchanging charged pions governs the largeness of reaction cross section. This is specific character of “nuclear reactions in condensed matter”.

### 1.3 Optical Potential

Global optical potential<sup>6)</sup>, written by complex number, is used for nuclear potential of strong interaction for scattering and sticking forces. Image of global optical potential is drawn in Fig.1-2. The real part, namely deep trapping potential  $V(r)$  is a well with rather round shape near at surface of nucleus (Woods-Saxon type), but is approximated to be constant value  $V_0$  within in nucleus.

$$U(r) = V(r) + iW(r) \tag{1-1}$$

$V_0$  is about -25MeV for deuteron.  $V_0$  value saturates to about -50MeV for nuclei of  $A>24$ . Imaginary part  $W(r)$  corresponds to the interaction of charged-pion exchange, and locates near at surface ( $r = r_0$ ) to be approximated by delta-function  $W_0\delta(r-r_0)$ . When we use this delta-function approximation, fusion rate formula becomes simple.

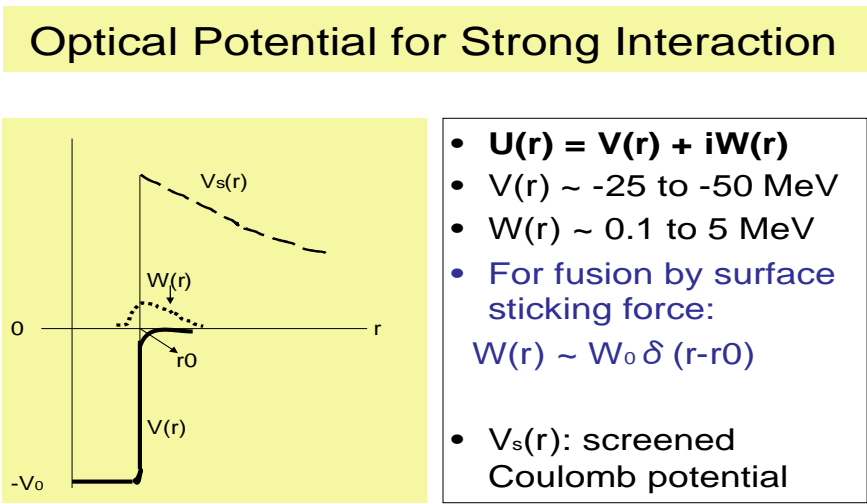


Fig.1-2: Optical potential for strong interaction

### 1.4 T Matrix and Reaction Cross Section

Now we briefly summarize quantum mechanical basis of scattering and reaction process.

Asymptotic wave function<sup>6,7)</sup> after scattering (interaction) is written by Eq.(2).

$$\Psi(r) \approx e^{ikz} + f(\theta)(e^{ikr}/r) \quad (1-2)$$

Differential cross section of process is defined by

$$\frac{d\sigma}{d\Omega} = |f(\theta)|^2 \quad (1-3)$$

S-matrix is defined by the phase-shift analysis<sup>6,7)</sup> as using Legendre polynomial expansion for scattering amplitude  $f(\theta)$ ,

$$f(\theta) = (1/2ik) \sum_{l=0}^{\infty} (2l+1)(S_l - 1)P_l(\cos\theta) \quad (1-4)$$

$$S_l = e^{2i\delta_l} \quad (1-5)$$

In general reaction process, not only elastic scattering but also absorption, fusion, particle emission processes are taking place as transition. To treat the transition from  $(\alpha, \beta)$  to  $(\alpha', \beta')$  channel, evaluation of T-matrix elements are usually done. T-matrix is defined<sup>7)</sup> by the following Lippmann-Schwinger equation,

$$T = U + UG_0T \quad (1-6)$$

$$G_0 = (E - H_0 + i\delta)^{-1} \quad (1-7)$$

$$H = U + H_0 \quad (1-8)$$

Here,  $G_0$  is the Green operator for  $H_0$  Hamiltonian with kinetic energy and spin Hamiltonian only.

Scattering amplitude is defined by,

$$f(\theta; \alpha\beta \rightarrow \alpha'\beta') = -(2\pi/\hbar^2) \langle \Psi_{\alpha'\beta'} | T | \Psi_{\alpha\beta} \rangle \quad (1-9)$$

If we approximate  $T=T^{(0)} = U$ , formula (1-9) becomes the Born approximation.

Lippmann-Schwinger equation can be regarded as an integral type equation of Schroedinger differential equation. The first order approximation of T is given by inserting  $T=U$  in Eq (1-6), and we get  $T^{(1)} = U + UG_0U$ . The second order approximation is then given as  $T^{(2)} = U + UG_0T^{(1)}$ , and the n-th order approximation gives  $T^{(n)} = U +$

$UG_0T^{(n-1)}$ . This successive treatment is known as Neumann series solution<sup>8)</sup> of integral equation.

We can treat reaction cross section including transition by evaluating T-matrix elements.

For the optical potential of  $V + iW$  type with constant  $V$  and  $W$  values, formulas of reaction cross section are given in standard text book of nuclear physics (Chapter 9 of Reference-6, for example) for S-wave ( $l = 0$ ).

$$\sigma_{r,0} = \pi\lambda^2 \frac{-4kR \operatorname{Im} f_0}{(\operatorname{Re} f_0)^2 + (\operatorname{Im} f_0 - kR)^2} \quad (1-10)$$

$$K = \frac{1}{\hbar} \sqrt{2M(E + V + iW)} \quad (1-11)$$

$$f_0 = KR \cot KR \quad (1-12)$$

And relations between S-matrix and T-matrix for Legendre coefficients are:

$$T_\ell = e^{i\delta_\ell} \sin \delta_\ell \quad (1-13)$$

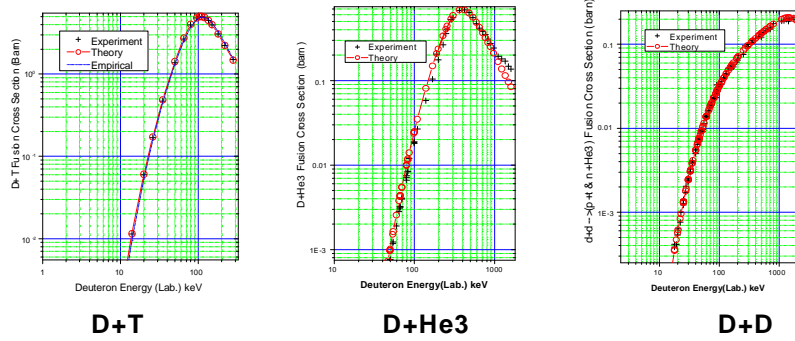
$$S_\ell = 1 + 2iT_\ell \quad (1-14)$$

By evaluating T-matrix elements, we can treat reaction with channel transition.

As shown in Figs.1-3 and 1-4, X. Z. Li evaluated<sup>9)</sup> fusion cross section for dd, dt and  $d^3\text{He}$  reactions using S-matrix formulas. Fusion cross sections are shown in Fig.1-3. S-matrix formula and evaluated values of  $V$  and  $W$  (written as  $U_{1r}$  and  $U_{1i}$  in Fig.1-4) for dt reaction are shown in Fig.1-4..

X.Z. Li: ICCF11

Selective Resonant Tunneling ○ & NNDC Data +



X. Z. Li, H.Hora, et al., *Laser and Particle Beam*, 22 No.4 (2004)

Fig.1-3: Fusion cross sections for dt, d<sup>3</sup>He and dd processes

Li used the reaction cross section formula with S-matrix elements as shown in Fig.1-4. He obtained averaged values of V and W of optical potential by fitting calculated curves to experimental cross sections.

Li: ICCF11

$$S_0 = e^{i2\delta_0} \quad \text{Cot}(\delta_0) = W_r + iW_i$$

$$\sigma_r^{(0)} \approx \frac{\pi}{k^2} (1 - |S_0|^2) \equiv \frac{\pi}{k^2} \left\{ \frac{-4W_i}{W_r^2 + (W_i - 1)^2} \right\}$$

Reaction Cross Section

$$\begin{cases} W_r = 0 \\ W_i = O(-1) \end{cases}$$

$$\begin{cases} E = 110 \text{ keV} \\ \sigma_r^{(0)} = 5.01 \text{ b} \end{cases} \quad \begin{cases} U_{1r} = -47.33 \text{ MeV} \\ U_{1i} = -115.25 \text{ keV} \end{cases}$$

$$a = 1.746 \times 10^{-13} (A_1^{1/3} + A_2^{1/3}) \text{ cm}$$

Fig.1-4: Fitting of dt fusion cross sections by S-matrix formulas, by Li<sup>9</sup>.

As explained in nuclear physics text books<sup>6</sup>, S-matrix elements by the phase-shift analysis can be used for estimating not only elastic scattering cross section but also total reaction cross section. However, the phase-shift analysis does not give information

on out-going channels and products by final state interaction.

### 1.5 Imaginary Part of Optical Potential

Now we move to the explanation of physical meaning for the imaginary part  $W$  of optical potential. From the conservation of quantum mechanical probabilistic density flow (a kind of continuity equation), we can take meaning of the imaginary part.

The forward Schroedinger equation is:

$$i\hbar \frac{\partial \Psi}{\partial t} = \left[ -\frac{\hbar^2}{2M} \nabla^2 + V + iW \right] \Psi \quad (1-15)$$

and the backward or adjoint equation is:

$$-i\hbar \frac{\partial \Psi^*}{\partial t} = \left[ -\frac{\hbar^2}{2M} \nabla^2 + V - iW \right] \Psi^* \quad (1-16)$$

Here we used complex conjugate potential for the adjoint (backward) equation.

We multiply  $\Psi^*$  on Eq.(1-15) from the left side, multiply  $\Psi$  on Eq.(1-16) from the left side and make mutual subtraction to get for the left hand side:

$$i\hbar \left( \Psi^* \frac{\partial \Psi}{\partial t} + \Psi \frac{\partial \Psi^*}{\partial t} \right) = i\hbar \frac{\partial \Psi \Psi^*}{\partial t} = i\hbar \frac{\partial \rho}{\partial t} \quad (1-17)$$

$$\text{Here, } \rho = \Psi \Psi^* \quad (1-18)$$

And we get for the right hand side:

$$i\hbar \frac{\partial \rho}{\partial t} = -\frac{\hbar^2}{2M} \left[ \Psi^* \nabla^2 \Psi - \Psi \nabla^2 \Psi^* \right] + i[2W\rho] = -i\hbar \text{div} \vec{j} + i[2W\rho] \quad (1-19)$$

Here we used formulas of quantum mechanical current flow as,

$$\begin{aligned} \vec{j} &= \frac{\hbar}{2im} (\Psi^* \vec{\nabla} \Psi + \Psi \vec{\nabla}^* \Psi^*) \\ &= \frac{\hbar}{2im} (\Psi^* \vec{\nabla} \Psi - \Psi \vec{\nabla} \Psi^*) \end{aligned} \quad (1-20)$$

$$\begin{aligned}
div\vec{j} &= \frac{\hbar}{2im}(\vec{\nabla}(\Psi * \vec{\nabla}\Psi) - \vec{\nabla}(\Psi\vec{\nabla}\Psi*)) \\
&= \frac{\hbar}{2im}(\Psi * \nabla^2\Psi + (\vec{\nabla}\Psi*)(\vec{\nabla}\Psi) - \Psi\nabla^2\Psi * -(\vec{\nabla}\Psi)(\vec{\nabla}\Psi*)) \\
&= \frac{\hbar}{2im}(\Psi * \nabla^2\Psi - \Psi\nabla^2\Psi*)
\end{aligned} \tag{1-21}$$

Consequently we obtain the modified continuity equation for probabilistic density flow:

$$\frac{\partial\rho}{\partial t} = -div(\vec{j}) + \frac{2}{\hbar}W\rho \tag{1-22}$$

It is obvious that the second term of Eq.(1-22) corresponds to the absorption rate term of the balance. (We do not have the second term in the continuity equation of fluid.)

Mean free path of particle in the strong force field of optical potential is given as (velocity)x(life-time), namely:

$$\Lambda = (\hbar/2)v/W(r) \tag{1-23}$$

### 1.6 Fusion Rate for Steady Molecule

Now we move to formulate fusion rate formulas for pseudo-molecule (EQPET molecule)<sup>10-19</sup> of two deuterons and bosonized electrons (quasi-particle)  $e^*(m/m_e, Z)$ . Here,  $m_e$  is the electron mass and  $Z$  is number charge of quasi-particle.

For deriving the trapping Coulomb potential, we will treat it later. Here, we assume an EQPET molecule is trapped in a shielded Coulomb potential similar to the Morse potential<sup>8</sup>. We illustrate the image of shielded Coulomb potential  $V_s(r)$  with optical potential in Fig.1-5. Scales are deformed for easy understanding the feature.

Range of strong nuclear force is very short in several fm region, and concentrated in near surface ( $r = r_0$ ) of nucleus. On the other hand, Coulomb interaction as electro-magnetic force distributes from  $r_0$  to nm long region effectively.

As a result, fusion rate for low energy under the strong interaction at around  $r=r_0$  can be treated by adiabatic approximation (namely Born-Oppenheimer approximation in quantum mechanics) to take product of the absorption rate by nuclear optical potential (imaginary part) and the tunneling probability of dd pair at  $r = r_0$ .

Fusion rate per dd pair is therefore defined as,

$$\lambda_{dd} = Tn|\Psi(r_0)|^2 \tag{1-24}$$

$$Tn = (2/\hbar)\langle\Psi_f|W(r)|\Psi_i\rangle \tag{1-25}$$

Here,  $|\Psi(r0)|^2$  is equivalent to the quantum mechanical tunneling probability of dd pair through the shielded Coulomb potential  $V_s(r)$ , as given by the WKB approximation<sup>7)</sup>. Fusion rate for muonic molecule  $dde^*(208,1)$  can be approximately given by Eq.(1-24), assuming the life time of muon is long enough. Actually the life time of muon is 2.2 micro-sec, and trapping potential should be regarded as adiabatic.

### 1.7 Fusion Rate for Dynamic Process

For more transient and dynamic process than muonic dd molecule, it is better to use formulas (Fermi's second golden rule) for cross section. Especially, for fusion rate calculations of EQPET molecules  $dde^*(2,2)$ ,  $dde^*(4,4)$ ,  $dde^*(6,6)$ ,  $dde^*(8,8)$ , lifetimes of pseudo-molecules are much shorter (assuming on the order of femto-sec) than muonic dd molecule.

Fusion rate is formulated as,

$$\lambda = \sigma v = (1/\hbar)vT^2\rho(E') \quad (1-26)$$

$$T = \langle \Psi_f | H_{\text{int}} | \Psi_i \rangle \quad (1-27)$$

Here  $v$  is the relative velocity for d-d interaction,  $\rho(E')$  is the final state density, and  $H_{\text{int}}$  is the effective interaction Hamiltonian as given by the approximate solution of Lippmann-Schwinger equation.

## Steady State Molecule $dde^*$

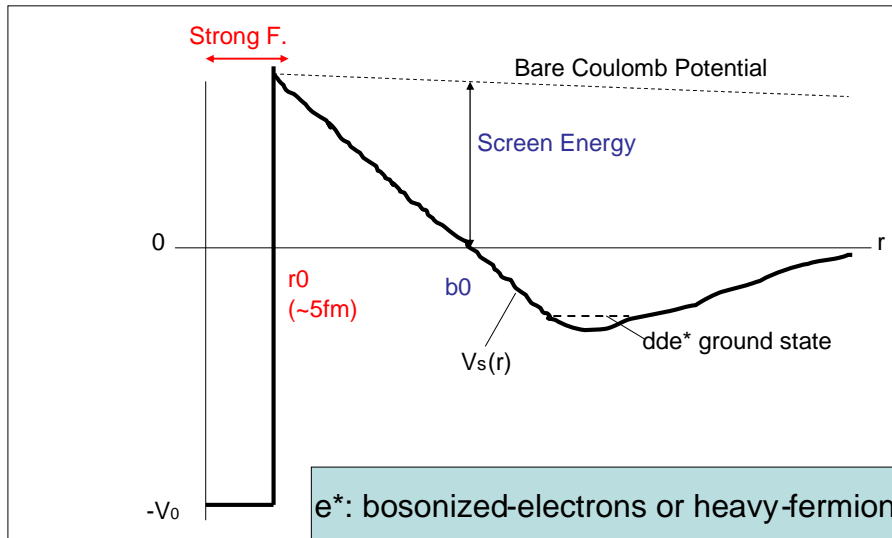


Fig.1-5: Trapping Coulomb + strong force potential for steady EQPET molecule of  $dde^*$

Fusion rate per  $dd$  pair is given by  $\langle \sigma v \rangle$ . Cross section  $\sigma$  is proportional to the square of T-matrix. To evaluate T-matrix elements, we need to treat many steps of physics as the formation process of EQPET  $dde^*$  molecule by the consequence of electromagnetic interaction in ordered (or constrained) space in condensed matter – solid state physics calculation of dynamic behavior of deuterons in lattice Bloch potential, atomic physics calculation to evaluate shielded Coulomb potential  $V_s(r)$  and strong interactions by global optical potential. After that, we need to evaluate the intermediate compound state with excited energy and spin-parity state. Finally we have to evaluate out-going channels and branching ratios of the final state interaction. In every step, we need to evaluate T-matrix elements.

## Part-II: Example - EQPET/TSC Model

### 2.1 Tetrahedral Symmetric Condensate (TSC)

As a seed of cold fusion or more extendedly condensed matter nuclear effects, a charge-neutral entity (pseudo-particle) of Platonic regular polyhedron composed with alternative positioning of deuteron (or proton) and electron at vertex of polyhedron has been proposed<sup>9-19</sup>. A representative one is the tetrahedral symmetric condensate (TSC) which is composed of 4 deuterons forming a regular tetrahedron and 4 electron balls also forming a regular tetrahedron. Each particle or ball sits at vertexes of cube. An electron ball at vertex depicts effective electron center of coupled two electrons having opposite spins each other. TSC is a transient pseudo-particle with short life (on the order of 100 fs at shortest). Exact place and condition for TSC production is still open question, but two models were proposed<sup>11-17</sup>. One (Model A) is the transient formation of TSC at T-sites of PdD under D-phonon excitation. The other (Model B) is the resonant coupling of two D<sub>2</sub> molecules at some focal points (corner hole, defect, etc) in near surface of metal-deuteride. TSC can make time-dependent squeezing motion under three-dimensional constraint to condensate at central focal point to become transiently a very small (on the order of 10 fm) charge-neutral pseudo-particle, which will make self-fusion of 4 deuterons within strong interaction (charged-pion exchange) range or will make deuteron-cluster-capture reaction with host metal nucleus<sup>11-17</sup>.

Estimation of fusion rate by the TSC squeezing motion has been formulated by evaluating T-matrix elements in three adiabatic steps, as illustrated in Fig.2-1. The first adiabatic process is for estimating D-cluster formation probability in condensed matter.

$$F_{nd} = \langle \Psi_1^2 \rangle \langle \Psi_2^2 \rangle \langle \Psi_3^2 \rangle \langle \Psi_4^2 \rangle \dots \langle \Psi_n^2 \rangle \quad (2-1)$$

where  $\Psi_n$  is the "lattice" wave function for the n-th deuteron. To estimate the D-cluster formation probability  $F_{nd}$  is most important for predicting experimental conditions. However practical modeling is of open question for future research.

The second adiabatic process is for estimating quantum mechanical barrier penetration probability  $P_B$ .  $P_B$  is approximately given by the WKB method<sup>7</sup>) as,

$$P_B = \exp(-n\Gamma_n) \quad (2-2)$$

where  $\Gamma_n$  is Gamow integral for n-deuterons cluster and given as,

$$\Gamma_n = (\sqrt{2\mu} / h) \int_{r_0}^b \sqrt{V_s(r) - E_d} dr \quad (2-3)$$

Here  $\mu$  is the reduced mass and  $r_0$  and  $b$  are given in Fig.1-5. For very low energy

fusion reaction,  $b$  is approximately given by  $b_0$ . Once the adiabatic screened potential, as illustrated in Fig.1-5, is calculated, for example as we show later by the EQPET model<sup>11-19</sup>), the Gamow integral can be numerically obtained by Eq.(2-3). The barrier penetration probability for multi-body fusion process is given in Eq.(2-2) by assuming that multi-body interaction takes place as very rapid cascade process of two-body interactions.

The third adiabatic process is for estimating cross section of multi-body strong interaction. Instead of evaluating T-matrix directly, it is more practical to use S-value, the astrophysical S-value, to write fusion cross section by strong interaction only as,

$$\sigma_{strong} = S_{nd} / E_d \tag{2-4}$$

Pure theoretical estimation of S-values for multi-body interaction is difficult because of so many-body (exchanging more than 6 charged pions for 3d, 4d, 6d and 8d fusion) problem. We introduce instead an empirical extrapolation as shown later.

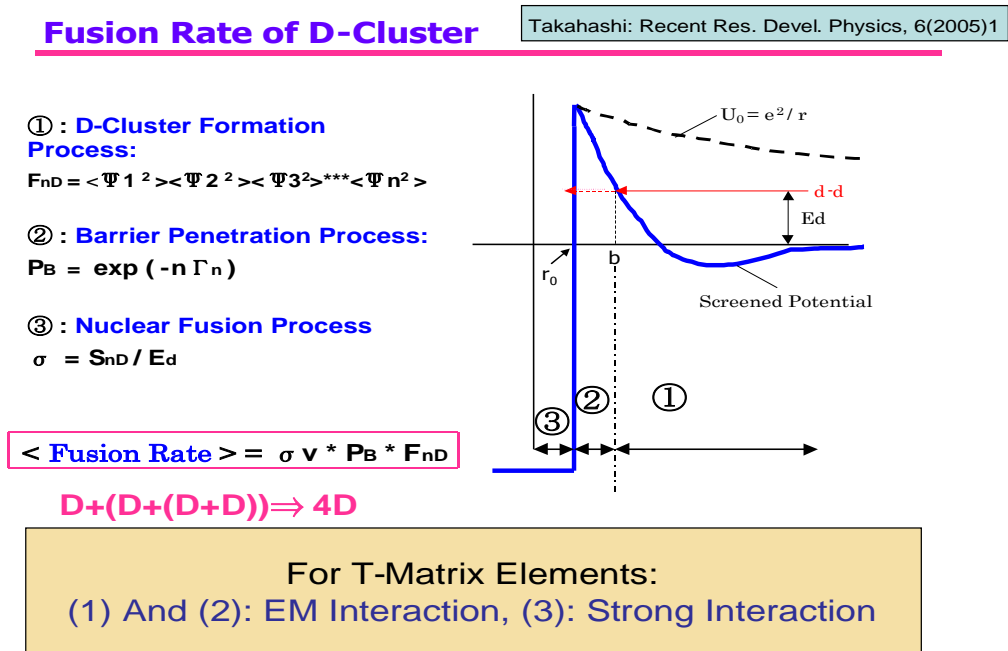
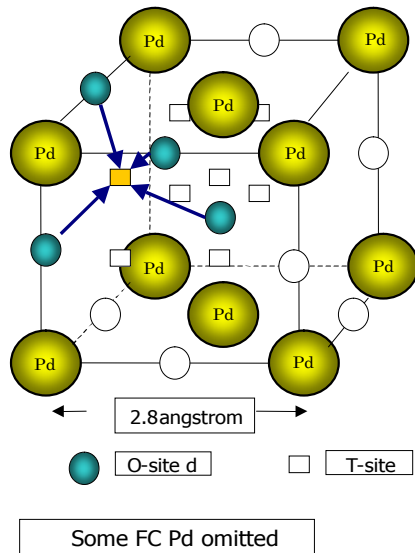


Fig. 2-1: Three adiabatic steps for formulating fusion rate in condensed matter

Model A for TSC formation is illustrated in Fig.2-2. We assume local fulfillment of  $x=1$  for PdDx lattice. We do not necessarily require the  $x=1$  condition (full D-loading) for bulk Pd sample. The local  $x=1$  condition may be fulfilled in near surface zone of Pd sample in experiment. Then we assume that D-in lattice is excited to higher phonon energy state by external stimulation. Laser beam irradiation on Pd sample surface may be a stimulation method for optical phonon excitation. It is known that D in PdDx lattice sits as Harmonic oscillator with  $\hbar\omega = 64meV$ , and  $E_0 = 32meV$ .

## Tetrahedral Condensation of D-Cluster



**Transient Bose  
Condensation of Deuterons**

**From O-site to T-site**

**Associating Transient  
Squeezing (**Bosonozation**)  
of 4d-shell Electrons**

**Generation of Short-Life  
Quasi-Particle  $e^*$  like  
Cooper-pair**

**D-Cluster as Mixture of  
 $DDe, DDee, DDe^*, DDe^*e^*$**

Fig.2-2: Model-A for TSC formation in PdD lattice under D-phonon excitation

As a function of phonon energy, we can estimate D-cluster formation probabilities at central T-sites, as example of such calculation is shown in Fig.2-4. However this process is essentially time-dependent (transient), and we have to treat more exactly the process as illustrated in Fig.2-3. We may first estimate the D-cluster formation probability within a small time-interval of “deep trapping hole” in Fig.2-3, by treating adiabatically the state (adiabatic  $dde^*$  state). Then we will make time-averaging for the periodical oscillation process. The adiabatic  $dde^*$  state is regarded as the most squeezed state (MSS). Numerical calculation for screened potential  $V_s(r)$  will be then done (shown later) by EQPET.

The example of D-cluster formation probability for Model A, as shown in Fig.2-4, is the treatment<sup>20)</sup> with quantum mechanical statistics, which does not include anti-parallel spin configuration for pairing electrons forming electron balls, neither treating the three dimensional constraint of squeezing motion under Platonic symmetry yet.

Centralized point-symmetric coherence of momentum-vectors for 4 deuterons and 4-electron balls is required to form TSC. This condition can not be expected in random motion of particles in plasma. The squeezing motion under three dimensional constraint (or ordering, or self-organization process) in lattice dynamics can realize that condition.

## D-Cluster Formation in PdD Transient Dynamics by Phonon Excitation

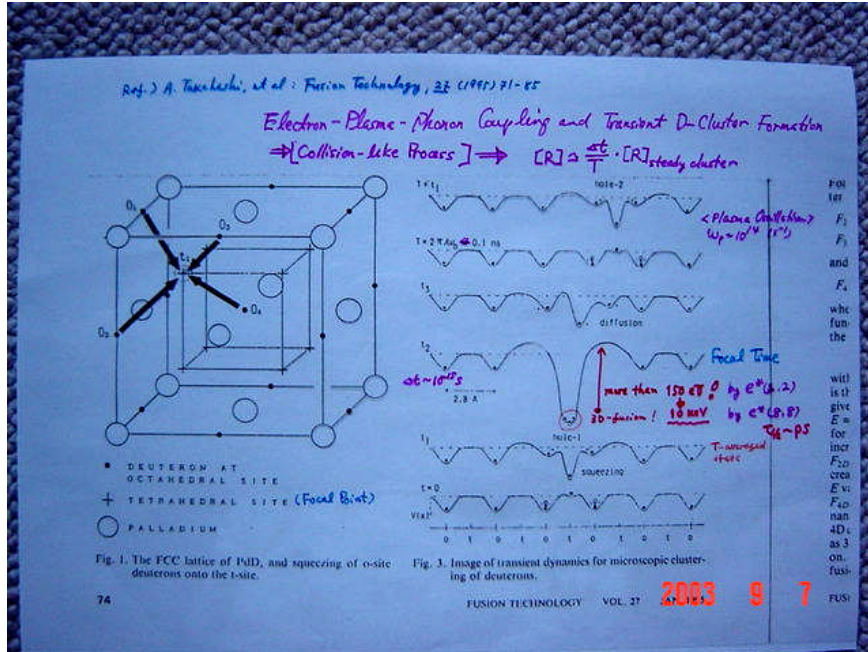
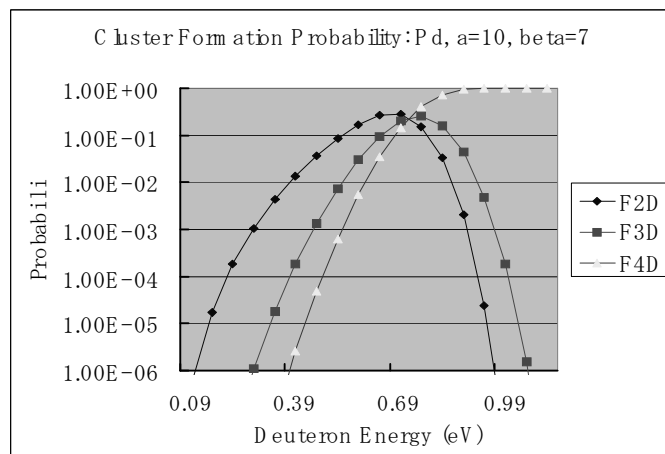


Fig.2-3: Image of lattice potential change by D-phonon excitation

### Cluster Formation Probability in Atomic Level



•Calculation by Excitation Screening Model

One Phonon Energy = 64 meV for D Harmonic Oscillator

Fig. 2-4: Example of estimation of D-cluster formation probability<sup>20)</sup>

**Tetrahedral Condensation of Deuterons in PdDx**

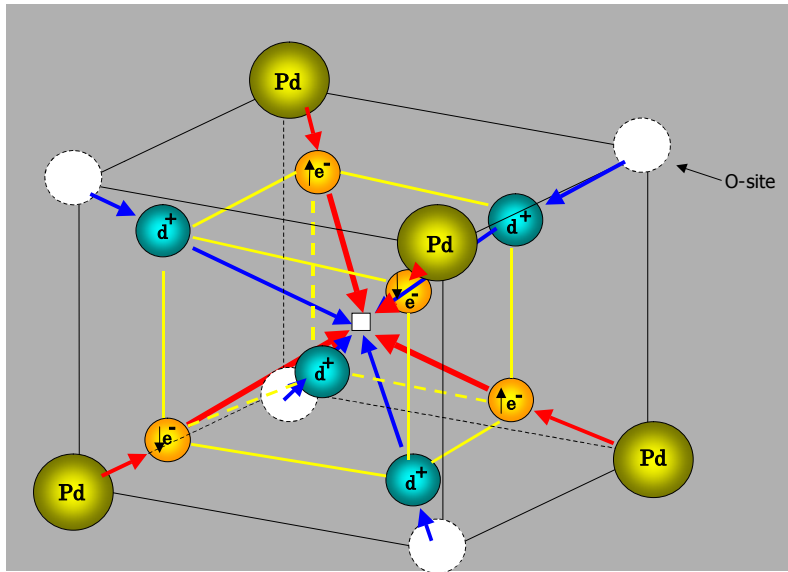
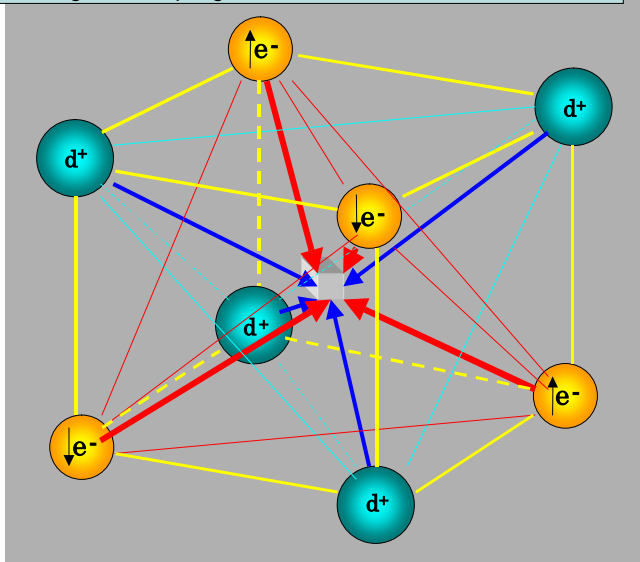


Fig. 2-5: Image of TSC formation in PdD lattice under statistical coherence by phonon excitation

**Classical View of Tetrahedral Sym. Condensation**

Orthogonal Coupling of Two  $D_2$  Molecule makes Miracle !



- Transient Combination of Two  $D_2$  Molecules (upper and lower)
- Squeezing only from O-Sites to T-site
- 3-dimension Frozen State for  $4d+s$  and  $4e-s$
- Quadruplet  $e^*$  (4,4)
- Formation of Electrons around T-site

Fig. 2-6: Semi-classical view of TSC (tetrahedral symmetric condensate) for 4 deuterons and 4 electron-balls (here electron balls are drawn as single electrons).

The semi-classical image of 4D cluster (TSC) is shown in Fig. 2-5. Pd atom has 10 outer

most electrons in 4d-shell. Pd atom is unique atom having largest number of valence electrons among atoms in nature. Electrons in 4d-shell contribute as quasi-free conduction-band electrons in Pd metal lattice.

Transition of physical system happens to realize the system-energy minimum state. The local energy minimum condition is formulated by the variational principle of quantum mechanics<sup>7,8</sup>. Eigen-value problem is led to solve secular equation.

However, under the ordering process (or self-organization process) in three dimensional constrained motion, the Platonic symmetry (regular polyhedron) for alternative positioning of deuteron (proton) and electron-ball makes obviously the averaged system electric charge zero. Namely TSC realizes minimum system Coulomb energy. Hence the TSC state can be a particular solution of variational method.

The semi-classical image of TSC is shown in Fig. 2-6. Pair of counter-part two electrons is the combination of anti-parallel spins, combination probability of which can be estimated simply. When momentum vectors of pairing two electrons are 180 degree opposite configuration, the transient Cooper pair  $e^*(2,2)$  is formed. Moreover, in TSC configuration, two Cooper pairs may couple orthogonally to form the quadruplet quasi-particle  $e^*(4,4)$ . As a general concept, this is the *bosonization* of electrons. Here, more exact quantum mechanical image for electron-ball is a pseudo-particle of 1/2 of coupling of two electrons with anti-parallel spin each other. More exact image is shown later in the time-dependent problem.

## 2.2 EQPET model

It is difficult to evaluate directly the total TSC wave function because of so many-body problem. The EQPET (electronic quasi-particle expansion theory) model assumes that the total TSC wave function can be written by the linear combination of partial wave functions for EQPET molecules  $dde^*$  for  $e^*(2,2)$  and  $e^*(4,4)$  and regular molecules  $dde$  ( $D_2^+$  ion) and  $ddee$  ( $D_2$  molecule).

$$|\Psi_N\rangle = a_1|\Psi_{(1,1)}\rangle + a_2|\Psi_{(2,2)}\rangle + a_4|\Psi_{(4,4)}\rangle + a_6|\Psi_{(6,6)}\rangle + a_8|\Psi_{(8,8)}\rangle \quad (2-5)$$

Here equation is written for including the case of OSC (octahedral symmetric condensate). For TSC,  $a_6$  and  $a_8$  are zero.

Fusion rate formula for  $dde^*$  is given<sup>11-19</sup> by,

$$\lambda_{(i,j)} = v(S_{2d}/E_d)\exp(-2\Gamma_{(i,j)}) \quad (2-6)$$

$$\Gamma_{(i,j)} = 0.218 \int_{r_0}^{b(i,j)} \sqrt{V_{s(i,j)}(R_{dd}) - E_d} dR_{dd} \quad (2-7)$$

Here  $R_{dd}$  is the inter-nuclear distance between two deuterons in D-cluster.

The modal fusion rate for TSC system is given by,

$$\lambda_N = a^2 \lambda_{(1,1)} + a^2 \lambda_{(2,2)} + a^4 \lambda_{(4,4)} + a^6 \lambda_{(6,6)} + a^8 \lambda_{(8,8)} \quad (2-8)$$

Formulas for screened Coulomb potentials  $V_s$  of EQPET molecules were given<sup>11-19</sup> by applying the solution for  $D_2^+$  ion and  $D_2$  molecule, based on the variational method<sup>21</sup>, as for  $dde^*$ ,

$$V_{s(i,j)} = \frac{e^2}{R_{dd}} + V_h + \frac{J + K}{1 + \Delta} \quad (2-9)$$

$$V_h = -13.6(e^*/e)^2(m^*/m_e) \quad (2-10)$$

Here  $V_h$  is the virtual binding energy of EQPET atom  $de^*$ . And,

$$i = e^*/e \quad (2-11)$$

is the number charge of  $e^*$ , and

$$j = m^*/m_e \quad (2-12)$$

The Coulomb integral  $J$  is given as,

$$J = (Ze^2/a_B) \left[ -\frac{1}{y} + \left(1 + \frac{1}{y}\right) \exp(-2y) \right] \quad (2-13)$$

The electron exchange integral  $K$  is given by,

$$K = (Ze^2/a_B)(1 + y) \exp(-y) \quad (2-14)$$

The non-orthogonal integral is,

$$\Delta = \left(1 + y + \frac{y^2}{3}\right) \exp(-y) \quad (2-15)$$

with

$$y = R_{dd}/(a_B/Z/(m^*/m_e)) \quad (2-16)$$

Here  $aB = a_B / Z / (m^* / m_e)$ ,  $a_B$  is Bohr radius (52.9 pm) and  $Z=e^*/e=i$ .

Fusion rate for multi-body reaction is given approximately by,

$$\lambda_{nd(i, j)} = v(S_{nd} / E_d) \exp(-n\Gamma(i, j)) \tag{2-16}$$

Modal fusion rate of multi-body fusion for TSC is then given by,

$$\lambda_{Nnd} = \sum_i a_i^2 \lambda_{nd(i, i)} \tag{2-17}$$

Calculated results of screened Coulomb potentials for EQPET molecules are shown in Fig. 2-7 and Fig.2-8.

### Screening Effect by EQPET Molecules

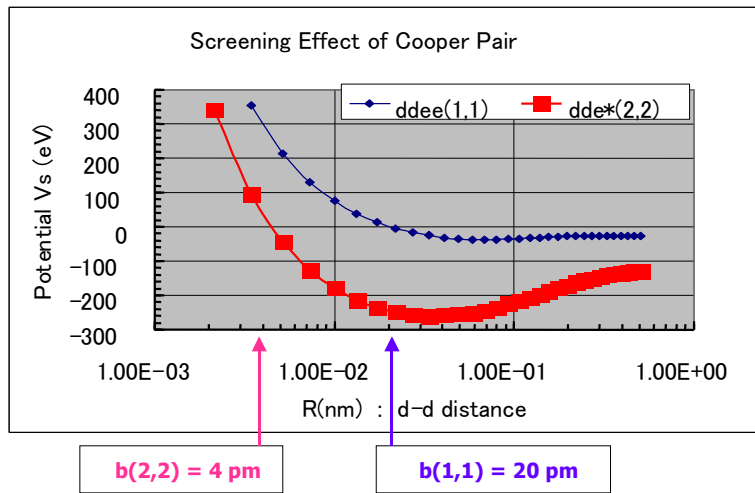


Fig. 2-7: Screened Coulomb potential for ddee ( $D_2$  molecule) and dde\*(2,2) (EQPET molecule with Cooper pair); change of b-parameter with deepening of negative potential depths results in condensing force for dde\* pseudo-molecule.

### Screening Effect: EQPET Molecule vs. Heavy Fermion

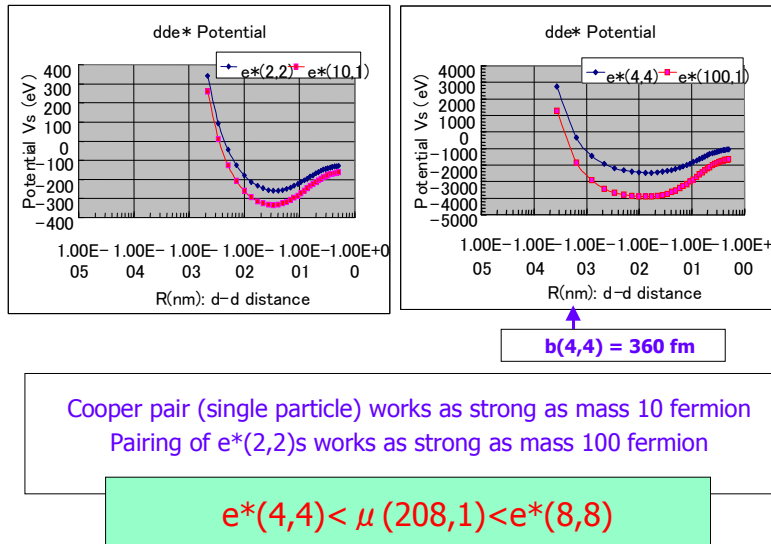


Fig.2-8: Comparison of screened Coulomb potentials between EQPET molecules and virtual molecules with heavy fermions; muon works as much as  $e^*(6,6)$ , c.f. Table 2-1.

### Screening Energy of EQPET Molecules

$U_s = -e^2/b_0$  for  $V_s(b_0) = 0$

	$U_s$ (eV)	$U_s$ (eV)	$b_0$ (pm)	$b_0$ (pm)
$e^*$	dde*	dde*e*	dde*	dde*e*
(1,1)	36	72	40	20
(2,2)	360	411	4	3.5
(4,4)	4,000	1,108	0.36	1.3
(8,8)	22,154	960	0.065	1.5
(208,1)	7,579	7,200	0.19	0.20
(6, 6)	9,600		0.15	

Table 2-1: Calculated screening energies by EQPET model

## Parameters of dde\* potentials

$e^*(m, Z)$	$V_{SMIN}$ (eV)	$b_0$ (pm)	$R_{dd}(gs)$ (pm)
(1, 1)	- 15.4	40	101
(1, 1)x2; D <sub>2</sub>	- 37.8	20	73
(2, 2)	- 259.0	4	33.8
(4, 4)	- 2,460	0.36	15.1

Trapping  
Depth

Ground  
State

Table-2-2: Main parameters of screened Coulomb potentials

Compared to the bare Coulomb potential, a low energy d-d pair can come closer to the position  $b_0$  classically and then penetrates quantum mechanically to the point  $r = r_0$  of strong interaction range. It is well known that muonic molecule  $dde^*(208,1)$  realize large dd fusion rate. Shielded Coulomb potential for  $dde^*(4,4)$  is equivalent to the one for  $dde^*(100,1)$ , and  $dde^*(6,6)$  has almost the same shielded Coulomb potential as muonic molecule. Here muon mass is used 207 plus 1 considering one electron added.

Screening energy by  $e^*$  is estimated by calculating bare Coulomb energy at  $r=b_0$ . Calculated screening energies are given in Table-2-1.

### 2.3 Multi-Body Strong Interaction

Now we move to explain the empirical formulas for extrapolating S-values of intrinsic cross section terms of two-body and multi-body strong interaction in fusion reaction process.

Basic measure PEF (pion exchange force) is defined as the scale of effective surface area for very short range attractive force, that is the catch-ball of charged pion between neutron-nucleon and proton-nucleon between two fusing nuclei. One PEF is defined as the number of string between n and p, as illustrated in upper figure of Fig.2-9.

As discussed in Part-I, sticking force of fusion happens at near surface of fusing nuclei. The larger is the sticking surface area, the larger is the fusion cross section. Using the PEF measure, PEF = 1 for HD fusion, PEF = 2 for DD fusion and PEF = 3 for DT fusion, respectively, as example for DD fusion is drawn in the lower figure of Fig.2-9.

Let us consider fusion reaction of deuteron with heavier nucleus, for example  ${}^6\text{Li} + d$  fusion. As drawn by the right figure of Fig.2-10, catch-ball of charged pions is interfered for about half of nucleons in  ${}^6\text{Li}$  nucleus due to self-shielding by more front nucleons. As

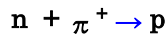
consequence of the self-shielding effect, PEF value would be around 3. For more heavy nuclei, PEF value should saturate to effective PEF values for interacting surface area.

On the contrary, multi-body deuteron fusion under the Platonic polyhedral configuration (e.g., regular tetrahedron for 4d fusion), there is no self-shielding effect. We can expect perfect exchange of charged pions among all deuterons of regular tetrahedral configuration as drawn in the left figure of Fig.2-10. Thus PEF =12 is given for 4d fusion. Similarly PEF =6 is given, for 3d fusion. We can say that effective sticking surface for multi-body fusion becomes very large as scaled by PEF number.

## Scaling of PEF (Pion Exchange Force) for Nuclear Fusion by Strong Interaction

---

Two Body Interaction: **PEF = 1**



(udd) (u**d\***) (uud) : u ; up quark



(uud) (**u\***d) (udd) : **u\*** ; anti-up quark

: **d\*** ; anti-down quark

For D + D Fusion; **PEF = 2**

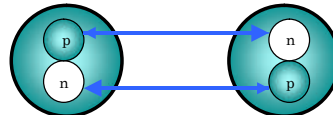
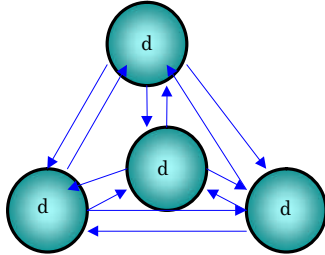


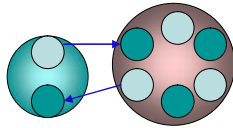
Fig.2-9: Definition of scaling measure PEF for fusion reaction

**4D →<sup>8</sup>Be\* vs. D+<sup>6</sup>Li → <sup>8</sup>Be\* ; for strong interaction**

**4D Fusion; PEF = 12**



**D + <sup>6</sup>Li Fusion: PEF = 2 + α**



4D Fusion has much larger Contact Surface of PEF than D+<sup>6</sup>Li with short range (few fm) charged-pion exchange

Fig.2-10: Estimation of effective sticking surface for fusion reactions, by the PEF measure for strength of charged pion exchange

Here we recognize that <sup>8</sup>Be\* is intermediate compound state both for the <sup>6</sup>Li + d and 4d reactions. And 4d fusion due to Platonic symmetry will have much larger cross section than the <sup>6</sup>Li + d reaction.

PEF values, hence fusion cross sections for 6d and 8d fusions in OSC condition may become much larger than 4d fusion.

Using known experimental S(0)-values for boson-related fusions, as pd, dd and dt fusion, we draw plot of S(0) values as a function of PEF value, and extrapolate to multi-body fusion using scaling formula, as shown in Fig.2-11. See also Fig.1-2.

$$S_n(0) \propto T_n^2 \propto (PEF)^N \tag{2-18}$$

Using S<sub>dd</sub> = 100 keVb and S<sub>dt</sub> = 2E+4 keVb, we estimated as scaling exponent N =11.4 and we got S<sub>4d</sub> = 1E+11 keVb.

### Effective S(0)-values for Multi-Body D-Fusion

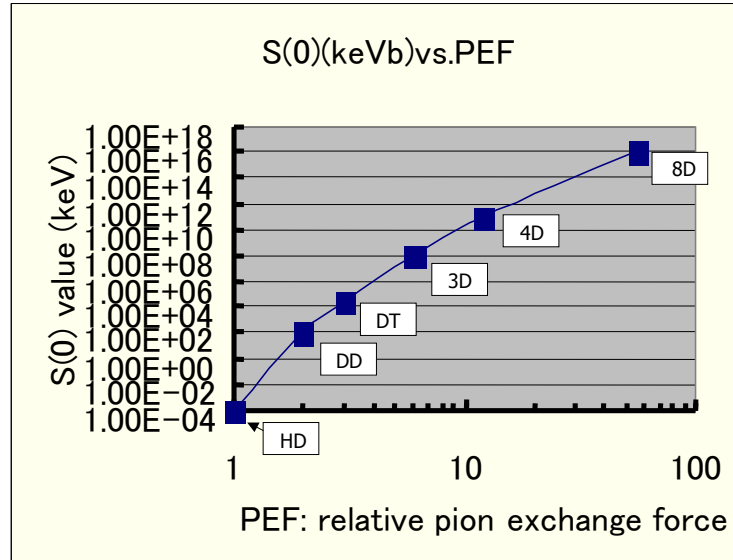


Fig.2-11: Empirical extrapolation of S(0) values as a function of PEF (effective sticking surface of fusion reaction) number, for multi-body fusion

Now we have finished preparation for fusion rate calculation. Calculated barrier penetration probabilities and fusion rates are shown in Table 2-3 for dde\* EQPET molecules.

### Barrier Factors (BF) and Fusion Rates (FR)

Ed = 0.22eV

(m*, e*)	Barrier Factor				Fusion Rate ( f/s/cl )			
	2D	3D	4D	8D	2D	3 D	4D	8D
(0,0)	E-1685				E-1697			
(1,1)	E-125	E-187	E-250	E-500	E-137	E-193	E-252	E-499
(2,1)	E-53	E-80	E-106	E-212	E-65	E-86	E-108	E-211
(2,2)	E-7	E-11	E-15	E-30	E-20	E-17	E-17	E-29
(4,4)	(3E-4)	E-5	E-7	E-14	(E-16)	E-11	E-9	E-13
(8,8)	(4E-1)	(2E-1)	(1E-1)	2E-2	(E-13)	(E-7)	(E-3)	E-1

( ) is virtual rate

Table 2-3: Calculated barrier factors and fusion rates (per cluster) for dde\*

### 2.4 Final State Interaction

Now we briefly summarize on the final state interactions and branching ratios to plural out-going channels.

The out-going break-up channels and branching ratios for dd fusion are very well established, as shown in Fig.2-12.

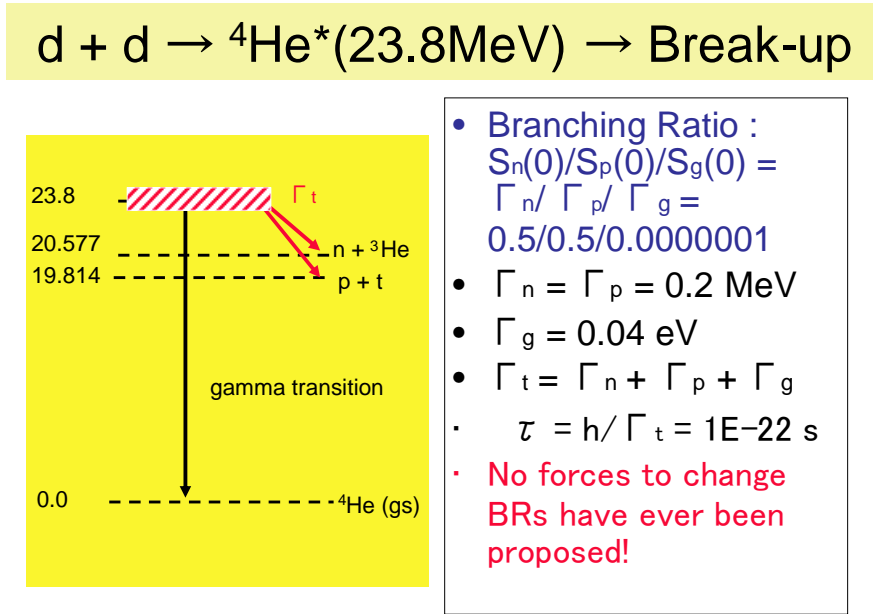
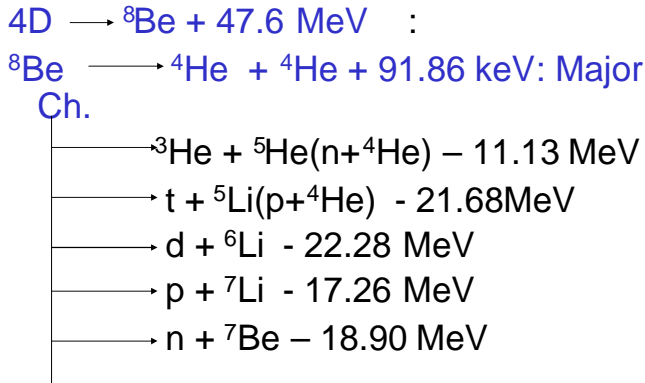


Fig.2-12: Final state interaction and branching ratios for dd fusion

Unless we could change the intermediate excited state  ${}^4\text{He}^*(Ex=23.8\text{MeV})$  by some external forces putting in (see the lower figure of Fig.2-9, for d-d reaction), we have no way to change the branching ratios. Namely, major channel for  ${}^4\text{He}$  generation never happens otherwise. The electromagnetic interaction (QED, phonon coupling, etc) is too weak to change the intermediate compound state. In the view of author, to put additional charged pion exchange into the d-d interaction by participating additional hadrons is actually possible way to get to the  ${}^4\text{He}$  production: however, this idea leads ones automatically to the multi-body (or cluster) fusion process.

In Fig.2-13, the final state interaction is drawn. The table of possible out-going channels is given in Table 2-4. The highly excited state  ${}^8\text{Be}^*$  can be regarded as a collectively deformed nucleus of two alpha-clusters, because of very hard formation of alpha-cluster in  ${}^8\text{Be}$  nucleus. The very high (47.6 MeV) excited energy is therefore rarely redistributed to single nucleon (n or p), or d, or t-cluster for particle emission.

## Decay-Channel of $^8\text{Be}$



**$^8\text{Be}$  Excited State may open to threshold reactions**

Table 2-4: All possible decay channels from  $^8\text{Be}^*$

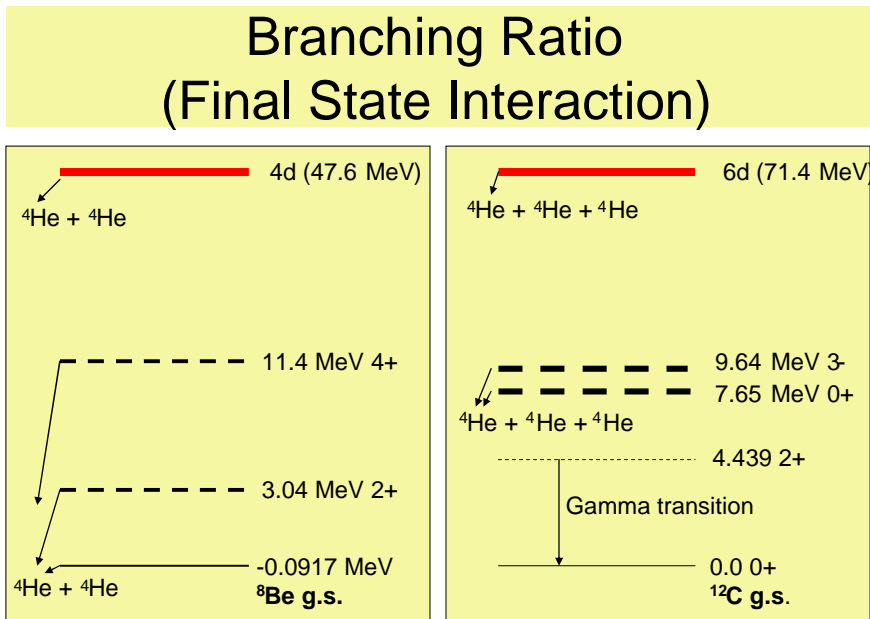


Fig.2-13: Final state interactions for 4d and 6d fusion reactions in condensed matter

We can speculate that all threshold reactions in Table 2-4 will not open in the final state interaction from 4d fusion, due to collective deformation of two alpha-clusters. Therefore,  $^8\text{Be}^*$  will decay with almost 100% weight to two  $^4\text{He}$  with 23.8 MeV kinetic energy per  $^4\text{He}$ , as illustrated in Fig.2-13. The decay channel of 6d fusion by OSC is also shown in the right figure of Fig.2-13.

We know that  $p + {}^7\text{Li}$  and  $n + {}^7\text{Be}$  channels appear in the  ${}^6\text{Li} + d$  beam-target reaction. We understand that these branches are caused by stripping reactions taking  $n$  or  $p$  from deuteron approaching to  ${}^6\text{Li}$  nucleus. The purely symmetric strong force exchange in the Platonic polyhedral condition, e.g. in the case of  $4d/\text{TSC}$  reaction in PdD lattice, ignores the stripping process.

### 2.5 Time-Dependent Approach

Detail of time-dependent analysis is given in Ref-19. Brief feature is illustrated in Fig.2-14. The semi-classical squeezing motion of TSC will get to its minimum size state with about 10 fm diameter in about 74 fs. Calculated effective time-interval for  $4d$  fusion is about 0.04 fs, namely very much short.

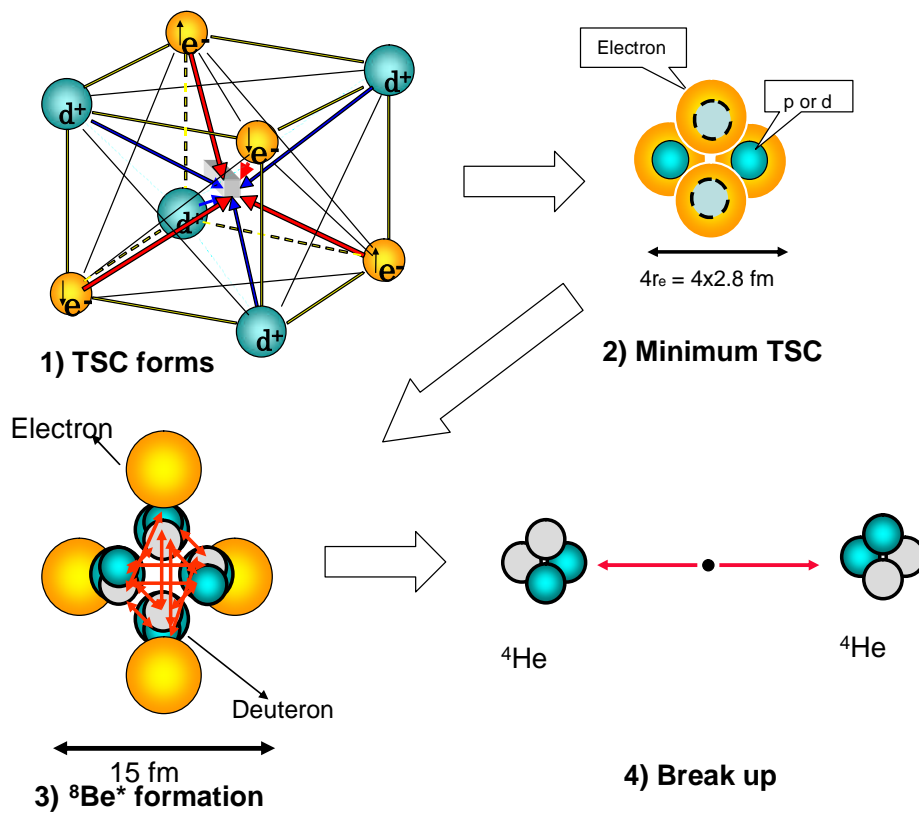
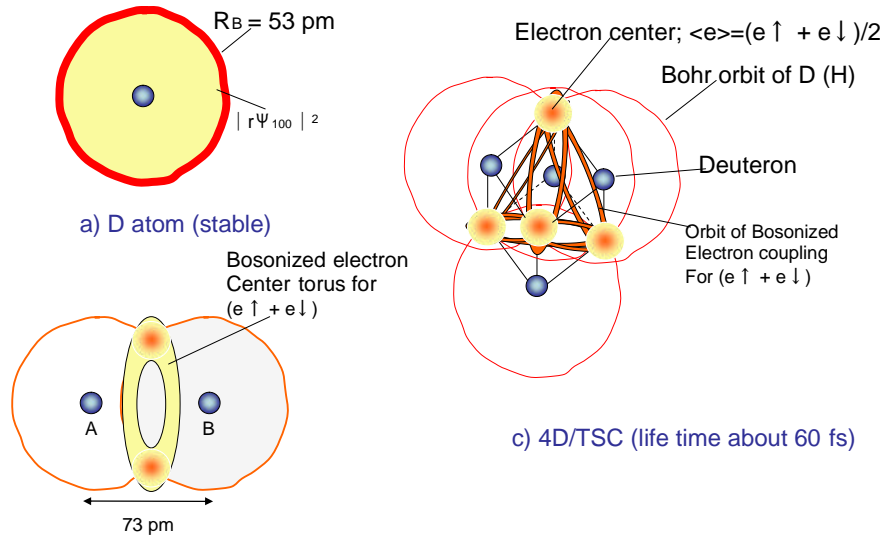


Fig.2-14: Semi-classical view of TSC squeezing motion and self-4d fusion reaction, here electron with spin should be electron-ball of 1/2 of two bosonized electrons in QM view.

Feature of QM Electron Cloud



b) D<sub>2</sub> molecule (stable):  $\Psi_{2D} = (2+2\Delta)^{-1/2} [\Psi_{100}(r_{A1}) \Psi_{100}(r_{B2}) + \Psi_{100}(r_{A2}) \Psi_{100}(r_{B1})] X_s(S1, S2)$

Fig.2-15: Initial state TSC wave function, compared with wave functions of D atom and D<sub>2</sub> molecule.

The TSC wave function at the starting point (t=0) can be drawn by superposition of 6 D<sub>2</sub> molecule wave functions on 6 surfaces of cube, as shown in c) of Fig.2-15. To calculate approximately time-dependent fusion rates, we can use adiabatic dde\* potentials, dividing into three time intervals for; normal electron state, Cooper pair state and quadruplet state respectively. For more accurate analysis, we need to develop an algorithm of molecular dynamics under three-dimensional constraint motion. This is our future task.

Time-dependent squeezing motion of TSC was first treated by the time-dependent EQPET (TDEQPET) model<sup>18)</sup>.

$$a_i \Psi_{4D}(r, t) = a_1 \Psi_{(1,1)}(r, t) + a_2 \Psi_{(2,2)}(r, t) + a_4 \Psi_{(4,4)}(r, t) \quad (2-19)$$

$$\langle r(t) \rangle = \langle r(0) \rangle - \langle v \rangle t \quad (2-20)$$

Because of the three-dimensionally and symmetrically constraint motion with averaged charge-neutrality for total TSC system, there is no force to stop squeezing motion until TSC size gets into the range of strong interaction (range of pion exchange). Therefore, the squeezing motion can be treated by the semi-classical Newtonian motion, as illustrated in Fig.2-16.

TSC Size by Dynamic Condensation in about 60 fs motion  
 - Semi-Classical Treatment Possible -

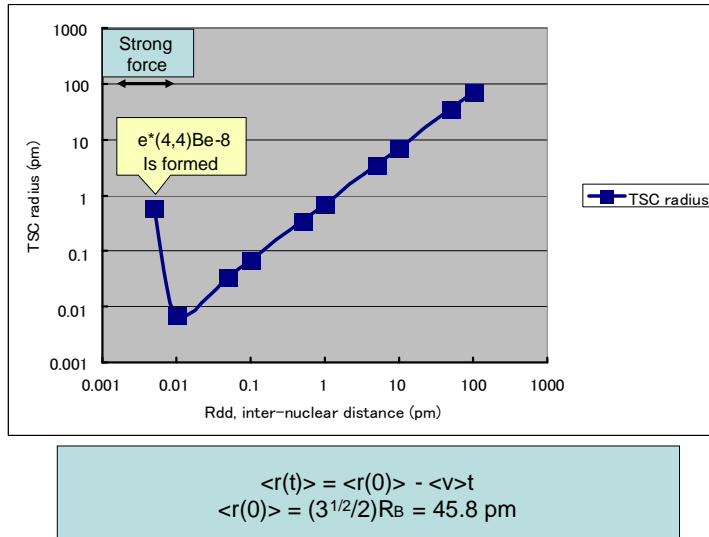


Fig.2-16: Linear decrease of TSC size by semi-classical Newtonian motion

To calculate time-dependent barrier penetration probability, we assumed that time-dependent change of potential can be replaced with three adiabatic potentials  $V_s$  for  $D_2$  molecule,  $dde^*(2,2)$  and  $dde^*(4,4)$  in three time intervals sequentially, according to the change of  $\langle r \rangle$  value comparing with  $b_0$ -parameters of adiabatic potentials..

Time dependent Gamow integral is defined as,

$$\Gamma(t) = 0.218 \int_{r_0}^{b(t)} \sqrt{V_s(R_{dd}) - E_d} dR_{dd} \quad (2-21)$$

Here  $b(t)$  is set to  $\langle r(t) \rangle$  for  $\langle r(t) \rangle > b_0$  parameter in each time interval for assumed adiabatic potential, namely  $e^*$  state.

Time dependent fusion rate were calculated, as shown in Fig.2-17. Time-averaged fusion rates were obtained as listed in Table 2-4.

Maximum TSC density possibly produced in PdD lattice is on the order of  $1E+22$  TSC/cm<sup>3</sup>. Multiplying this number to cluster fusion rates in Table 2-4, we obtain dd fusion rate which emit neutrons on the order of  $3E-3$  ( $3 \times 10^{-3}$ ) n/s/cm<sup>3</sup>. This level of neutron emission is difficult to detect by usual detectors. On the contrast, we obtain 4d fusion rate as  $5.5E+14$  ( $5.5 \times 10^{14}$ )  $\alpha$  /s/cm<sup>3</sup> which corresponds to  $55 \text{ kW/cm}^3$  power level. Thus, neutron free clean fusion reaction producing large heat density and <sup>4</sup>He ash, as reported by experiments of Arata, McKubre, de Ninno, Violante, Isobe etc. can be now theoretically explained.

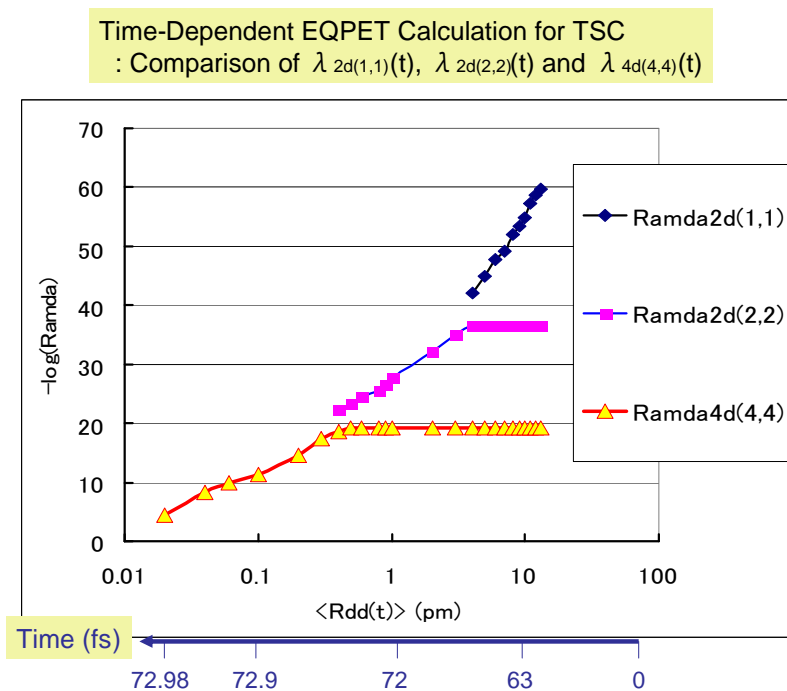


Fig.2-17: Calculated time-dependent fusion rates by TDEQPET model

**TDEQPET Cal. For EQPET Molecules**

$e^*(m, Z)$	$\langle \lambda_{2d} \rangle$ (f/s/cl.)	$\langle \lambda_{4d} \rangle$ (f/s/cl.)	$\lambda_{2d}(0)$ (f/s/cl.)	$\lambda_{4d}(0)$ (f/s/cl.)
(1, 1)	4.3E-44	7.8E-63	1.9E-60	7.3E-93
(2, 2)	2.9E-25	2.5E-24	2.4E-37	1.1E-50
(4, 4)	(2.1E-17)*	5.5E-8	(5.5E-22)*	5.9E-20

( )\* : virtual value

Table 2-4: Time-averaged fusion rates by TDEQPET model, compared with values at  $t=0$ .

[References]

- 1): J. M. Blatt, V. F. Weisskopf: **Theoretical Nuclear Physics**, Chapter VIII, Springer-Verlag, 1979
- 2): A. Takahashi, et al: *JJAP*, 41(2001)pp.7031-7046
- 3): M. Ohta, A. Takahashi: *JJAP*, 42(2002)pp.645-649
- 4): A. Takahashi: Theoretical backgrounds for transmutation reactions, ppt slides for Sunday School of ICCF10, see <http://www.lenr-canr.org/> Special Collection for ICCF10
- 5): B. Povh, K. Rith, C. Scholtz, F. Zetsche: **Teilchen und Kerne**, Springer, 1994
- 6): K. Yagi: **Nuclear Physics (in Japanese)**, Asakura, Tokyo, 1971
- 7): L. I. Schiff: **Quantum Mechanics**, McGraw-Hill (1955)
- 8): P. M. Morse, H. Feshbach; **Methods of Theoretical Physics**, McGraw-Hill (1953)
- 9): X. Z. Li, et al: *Phys. Rev. C*, 61(2000)24610
- 10): A. Takahashi: Condensed matter nuclear effects, Proc. Int. Meet. Frontiers of Physics, Kuala Lumpur, 25-29 July 2005, *Malaysian J. Physics*, to be published
- 11): A. Takahashi: Deuteron cluster fusion and related nuclear reactions in metal-deuterium/hydrogen systems, *Recent Res. Devel. Physics*, 6(2005)pp.1-28, ISBN: 81-7895-171-1
- 12): A. Takahashi: Proc. ICCF9, pp.343-348, see Ref-2
- 13): A. Takahashi: Mechanism of deuteron cluster fusion by EQPET model, Proc. ICCF10, see Ref-3
- 14): A. Takahashi: Proc. JCF5, 6, see <http://wwwcf.elc.iwate-u.ac.jp/jcf/>
- 15): A. Takahashi: Proc. ICCF11
- 16): A. Takahashi: Deuteron cluster fusion and ash, Proc. ASTI5 Meeting, see Ref-5
- 17): A. Takahashi: A theoretical summary of condensed matter nuclear effects, Proc. Siena2005 Workshop, see also A. Takahashi: Brief Theoretical Summary of Condensed Matter Nuclear Effects, *Acta Physica et Chemica*, Debrecen, Hungary, Vol.38-39, (2005)341-356
- 18): A. Takahashi: Time-dependent EQPET analysis of TSC, Proc. ICCF12, Yokohama 2005
- 19): C. J. Pethic, H. Smith; **Bose-Einstein condensation in dilute gases**, U. Chicago publ. (2001)
- 20): A. Takahashi, H. Numata, Y. Iwamura, H. Yamada, T. Ohmori, T. Mizuno, T. Akimoto: **"Nuclear Reactions in Solids" (in Japanese)**, Kogakusha, Tokyo, 1999
- 21): S. Shirato: **Atomic Physics-II (in Japanese)**, Nippon Rikou Publ. Tokyo, 1984